

# Heavy Higgs searches and constraints on two Higgs doublet models

Chien-Yi Chen and Sally Dawson

*Department of Physics, Brookhaven National Laboratory, Upton, New York 11973, USA*

Marc Sher

*High Energy Theory Group, College of William and Mary, Williamsburg, Virginia 23187, USA*

(Received 13 May 2013; published 12 July 2013; corrected 31 July 2013)

Since the discovery of a Higgs boson at the LHC and the measurement of many of its branching ratios, there have been numerous studies exploring the restrictions these results place on the parameter space of two Higgs doublet models. We extend these results to include the full data set and study the expected sensitivity that can be obtained with  $300 \text{ fb}^{-1}$  and  $3000 \text{ fb}^{-1}$  integrated luminosity. We consider searches for a heavy Standard Model Higgs boson, with a mass ranging from 200 to 400 GeV, and show that the nonobservation of such a Higgs boson can substantially narrow the allowed regions of parameter space in two Higgs doublet models.

DOI: [10.1103/PhysRevD.88.015018](https://doi.org/10.1103/PhysRevD.88.015018)

PACS numbers: 12.60.Fr

## I. INTRODUCTION

Following the discovery of a Higgs boson, experiments at the LHC can begin to probe the electroweak symmetry breaking sector. Their task is to measure the properties of the Higgs boson as precisely as possible. Any deviation from the Standard Model predictions would be evidence of physics beyond the Standard Model. Many extensions of the Standard Model have been proposed over the past few decades, and many contain an electroweak symmetry breaking sector with more than one Higgs doublet. These extensions can easily accommodate a 125 GeV scalar, but also typically predict deviations in its couplings. Thus, it is crucial to examine extensions of the Standard Model and determine the expectations for the couplings of the  $M_{h^0} = 125 \text{ GeV}$  scalar. Some of the simplest extensions of the scalar sector are the two Higgs doublet models (2HDMs) [1]. The 2HDMs contain five physical Higgs scalars: a charged Higgs  $H^\pm$ , a pseudoscalar  $A$ , and two neutral scalars,  $h$  and  $H$ . Although it is possible that the 125 GeV state is the heavier of the neutral scalars [2–4], we assume here that it is the lighter.

In general, 2HDMs have Higgs mediated tree level flavor changing neutral currents, which must be suppressed. Most 2HDMs eliminate flavor changing neutral currents by imposing a discrete  $Z_2$  symmetry in which the fermions of a given charge only couple to one of the Higgs doublets. The two most familiar versions are the type-I model, in which all of the fermions couple to the same Higgs doublet, and the type-II model, in which the  $Q = 2/3$  quarks couple to one doublet and the  $Q = -1/3$  quarks and leptons couple to the other. Two additional versions interchange the lepton assignments. In the “lepton-specific” model, all of the quarks couple to one doublet while the leptons couple to the other, and in the “flipped” model, the  $Q = 2/3$  quarks and leptons couple to one doublet and the  $Q = -1/3$  quarks couple to the other. All four of these models have been extensively

studied [1]. The couplings of the Higgs bosons to fermions are described by two free parameters. The ratio of vacuum expectation values of the two Higgs doublets is  $\tan \beta \equiv \frac{v_2}{v_1}$ , and the mixing angle which diagonalizes the neutral scalar mass matrix is  $\alpha$ . The couplings of the light (heavy)  $CP$ -even Higgs boson,  $h^0$  ( $H^0$ ), to fermions and gauge bosons relative to the Standard Model couplings are given for all four 2HDMs considered here in Tables I and II.

Following the initial evidence for a Higgs boson at  $M_{h^0} = 125 \text{ GeV}$ , Ferreira *et al.* [5] studied the implications of such a Higgs particle for the four versions of the 2HDMs and presented the expected branching ratios of the  $M_{h^0} = 125 \text{ GeV}$  state. Subsequently, many papers [6–22] examined various channels in the four 2HDMs in light of the experimental findings at the LHC. More recently, Ref. [23] updated the study of type-I and type-II models, using the entire LHC data set. In Sec. II, we update

TABLE I. Light neutral Higgs ( $h^0$ ) couplings in the 2HDMs.

	I	II	Lepton specific	Flipped
$g_{hVV}$	$\sin(\beta - \alpha)$	$\sin(\beta - \alpha)$	$\sin(\beta - \alpha)$	$\sin(\beta - \alpha)$
$g_{ht\bar{t}}$	$\frac{\cos \alpha}{\sin \beta}$	$\frac{\cos \alpha}{\sin \beta}$	$\frac{\cos \alpha}{\sin \beta}$	$\frac{\cos \alpha}{\sin \beta}$
$g_{hb\bar{b}}$	$\frac{\cos \alpha}{\sin \beta}$	$-\frac{\sin \alpha}{\cos \beta}$	$\frac{\cos \alpha}{\sin \beta}$	$-\frac{\sin \alpha}{\cos \beta}$
$g_{h\tau^+\tau^-}$	$\frac{\cos \alpha}{\sin \beta}$	$-\frac{\sin \alpha}{\cos \beta}$	$-\frac{\sin \alpha}{\cos \beta}$	$\frac{\cos \alpha}{\sin \beta}$

TABLE II. Heavy neutral  $CP$ -even Higgs ( $H^0$ ) couplings in the 2HDMs.

	I	II	Lepton specific	Flipped
$g_{HVV}$	$\cos(\beta - \alpha)$	$\cos(\beta - \alpha)$	$\cos(\beta - \alpha)$	$\cos(\beta - \alpha)$
$g_{Ht\bar{t}}$	$\frac{\sin \alpha}{\sin \beta}$	$\frac{\sin \alpha}{\sin \beta}$	$\frac{\sin \alpha}{\sin \beta}$	$\frac{\sin \alpha}{\sin \beta}$
$g_{Hb\bar{b}}$	$\frac{\sin \alpha}{\sin \beta}$	$\frac{\cos \alpha}{\cos \beta}$	$\frac{\sin \alpha}{\sin \beta}$	$\frac{\cos \alpha}{\cos \beta}$
$g_{H\tau^+\tau^-}$	$\frac{\sin \alpha}{\sin \beta}$	$\frac{\cos \alpha}{\cos \beta}$	$\frac{\cos \alpha}{\cos \beta}$	$\frac{\sin \alpha}{\sin \beta}$

previous studies [6] for all four 2HDMs to include the full data set and highlight the significant effect of the latest CMS result on  $h \rightarrow \gamma\gamma$  on the global fit. We extend previous results to demonstrate the expected sensitivity with  $300 \text{ fb}^{-1}$  or  $3000 \text{ fb}^{-1}$ . In Sec. III, we show that current ATLAS and CMS bounds on a *heavy* Higgs boson, with mass between 200 and 400 GeV, can bound regions of parameter space that have not yet been covered by the analysis of the  $M_{h^0} = 125 \text{ GeV}$  Higgs decays, and we extend these limits as well to  $300 \text{ fb}^{-1}$  and  $3000 \text{ fb}^{-1}$ .

## II. LHC REACH FROM $h^0$ MEASUREMENTS

Previous analyses examined individual decays of the  $M_{h^0} = 125 \text{ GeV}$  Higgs, the  $h^0$ , and looked at the implications for 2HDMs, finding the regions in the  $(\alpha, \beta)$  parameter space allowed by current LHC data. Reference [6] determined, for each of the four 2HDMs, the allowed regions of parameter space. We have updated their results to include the most recent experimental data and have also studied the bounds that can be obtained at a future LHC experiment with 14 TeV and integrated luminosities of  $300 \text{ fb}^{-1}$  and  $3000 \text{ fb}^{-1}$ . To estimate these bounds, we look at the current errors, assume that the Standard Model prediction is correct, and scale the errors as  $1/\sqrt{N}$ , where  $N$  scales like the integrated luminosity. This corresponds to ‘‘scheme 2’’ of the CMS [24] high luminosity projections [25].

A  $\chi^2$  fit to the data shown in Tables III and IV is performed assuming  $M_{h^0} = 125 \text{ GeV}$ . We follow the

TABLE IV. Measured Higgs signal strengths.

Decay	Production	Measured signal strength $R^{\text{meas}}$
$b\bar{b}$	Vh	$-0.4 \pm 1.0$ [ATLAS] [33]
	Vh	$1.3^{+0.7}_{-0.6}$ [CMS] [34]
	Vh	$1.56^{+0.72}_{-0.73}$ [Tevatron] [28]
$\tau^+\tau^-$	ggF	$2.4 \pm 1.5$ [ATLAS] [35]
	VBF	$-0.4 \pm 1.5$ [ATLAS] [35]
	inclusive	$0.8 \pm 0.7$ [ATLAS] [33]
	ggF	$0.73 \pm 0.50$ [CMS] [36]
	VBF	$1.37^{+0.56}_{-0.58}$ [CMS] [36]
	Vh	$0.75^{+1.44}_{-1.40}$ [CMS] [36]
	inclusive	$1.1 \pm 0.4$ [CMS] [36]
	ggF	$2.1^{+2.2}_{-1.9}$ [Tevatron] [28]

standard definition of  $\chi^2 = \sum_i \frac{(R_i^{\text{2HDM}} - R_i^{\text{meas}})^2}{(\sigma_i^{\text{meas}})^2}$ , where  $R^{\text{2HDM}}$  represents predictions for the signal strength from the 2HDMs and  $R^{\text{meas}}$  stands for the measured signal strength shown in Tables III and IV. When the errors are asymmetric, we have averaged them in quadrature,  $\sigma = \sqrt{\frac{(\sigma_+)^2 + (\sigma_-)^2}{2}}$ . Although including the asymmetric errors in the analysis would in general provide more accurate information, in this case the only data with substantial asymmetric errors are the CMS vector boson fusion channel with  $h^0 \rightarrow ZZ$  and the Tevatron gluon fusion channel with  $h^0 \rightarrow \tau^+\tau^-$ , both of which have relatively little pull on the overall  $\chi^2$ . Therefore this assumption will have only a very minor effect on our results.

Our results are given in Fig. 1. For each of the four models, we plot the current limits on the parameter space, and the projected limits for integrated luminosities of  $300 \text{ fb}^{-1}$  and  $3000 \text{ fb}^{-1}$ . Bounds from flavor physics constrain  $\tan\beta \geq 1$  [6,37] and we take this as a prior when we determine the chi-squared minima. In all of the models the minimum of the  $\chi^2$  occurs for  $\tan\beta \sim 1$  and  $\cos(\beta - \alpha) \sim 0$ , demonstrating that the couplings of a 2HDM are already constrained to be close to the Standard Model values. Similar bounds for the type-I and type-II models have been obtained in Ref. [38]. The parameter space for the type-I model is not very constrained at present. This is because, in the large  $\tan\beta$  limit, the Higgs is fermiophobic and production through gluon fusion is suppressed. Increasing the integrated luminosity will gradually narrow the allowed parameter space. The lepton-specific model is not severely constrained either because of the enhanced decay to  $\tau$  leptons, which is poorly measured at present. For large  $\tan\beta$ , the bottom-quark Yukawa coupling becomes substantial in the type-II and flipped models, and thus the currently allowed parameter space is much more restricted. We do not show a very small allowed (by LHC data) region in the lower right for  $\tan\beta \sim 0-0.5$  because that region is excluded by  $B$  physics constraints. For each of the models

TABLE III. Measured Higgs signal strengths.

Decay	Production	Measured signal strength $R^{\text{meas}}$
$\gamma\gamma$	ggF	$1.6^{+0.3+0.3}_{-0.3-0.2}$ [ATLAS] [26]
	VBF	$1.7^{+0.8+0.5}_{-0.8-0.4}$ [ATLAS] [26]
	Vh	$1.8^{+1.5+0.3}_{-1.3-0.3}$ [ATLAS] [26]
	inclusive	$1.65^{+0.24+0.25}_{-0.24-0.18}$ [ATLAS] [26]
	ggF + tth	$0.52 \pm 0.5$ [CMS] [27]
	VBF + Vh	$1.48^{+1.24}_{-1.07}$ [CMS] [27]
	inclusive	$0.78^{+0.28}_{-0.26}$ [CMS] [27]
	ggF	$6.1^{+3.3}_{-3.2}$ [Tevatron] [28]
	WW	ggF
VBF + Vh		$1.66 \pm 0.79$ [ATLAS] [29]
inclusive		$1.01 \pm 0.31$ [ATLAS] [29]
ggF		$0.76 \pm 0.21$ [CMS] [30]
ggF		$0.8^{+0.9}_{-0.8}$ [Tevatron] [28]
ZZ	ggF	$1.8^{+0.8}_{-0.5}$ [ATLAS] [31]
	VBF + Vh	$1.2^{+3.8}_{-1.4}$ [ATLAS] [31]
	inclusive	$1.5 \pm 0.4$ [ATLAS] [31]
	ggF	$0.9^{+0.5}_{-0.4}$ [CMS] [32]
	VBF + Vh	$1.0^{+2.4}_{-2.3}$ [CMS] [32]
	inclusive	$0.91^{+0.30}_{-0.24}$ [CMS] [32]

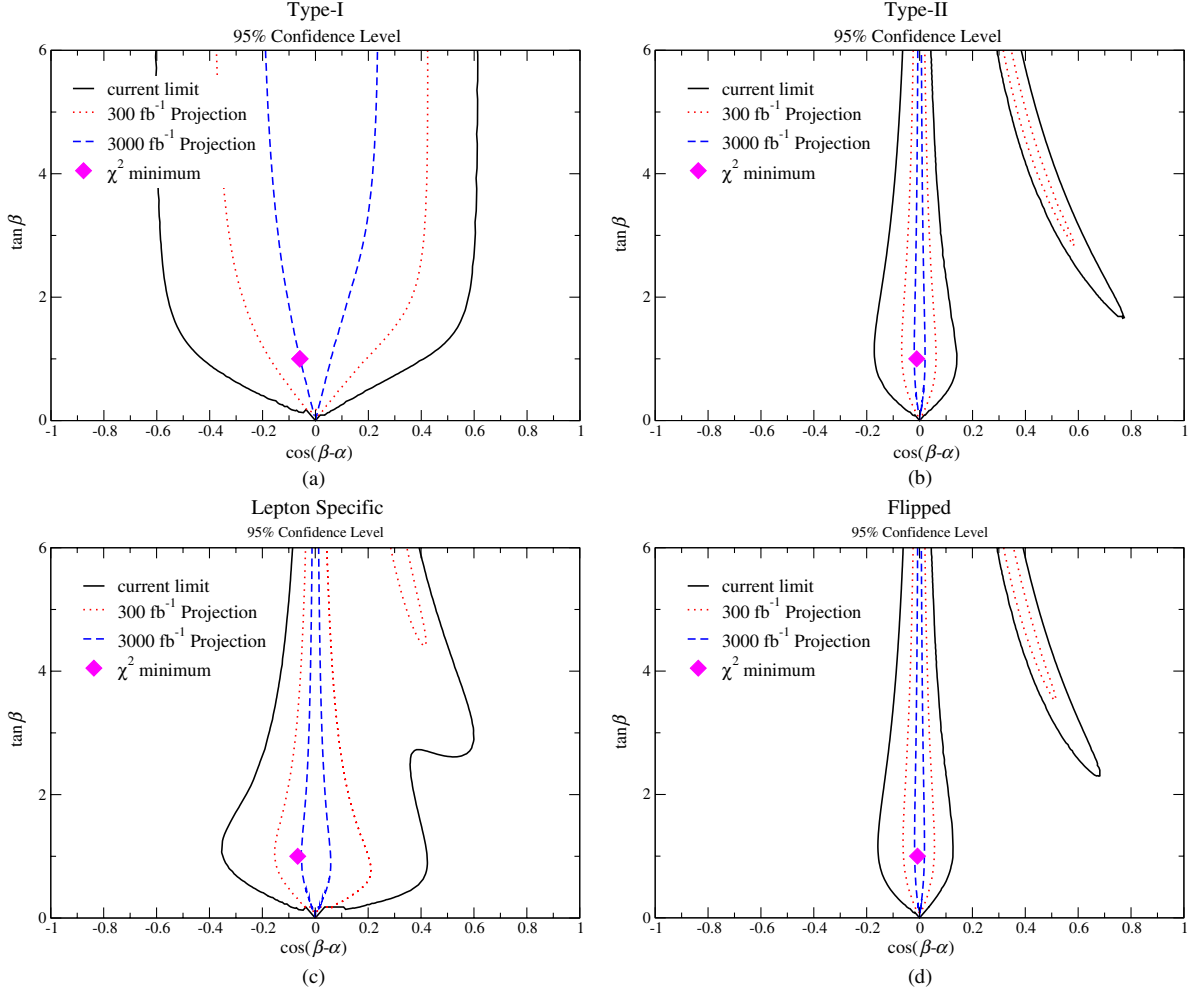


FIG. 1 (color online). Allowed regions in the  $(\cos(\beta - \alpha), \tan\beta)$  plane in type-I (a), type-II (b), lepton-specific (c), and flipped (d) 2HDMs obtained by performing a  $\chi^2$  analysis. The region between the black (solid), red (dotted), and blue (dashed) lines is allowed at 95% confidence level corresponding to the current limits and the projected limits for integrated luminosities of  $300 \text{ fb}^{-1}$  and  $3000 \text{ fb}^{-1}$ , respectively.

considered here, the measured value of  $\Delta M_{B_d}$  excludes such small values of  $\tan\beta$  [6].

The most general potential with two Higgs doublets,  $\Phi_1$  and  $\Phi_2$ , and a softly broken  $Z_2$  symmetry is

$$\begin{aligned}
 V = & m_{11}^2 \Phi_1^\dagger \Phi_1 + m_{22}^2 \Phi_2^\dagger \Phi_2 - \mu^2 (\Phi_1^\dagger \Phi_2 + \Phi_2^\dagger \Phi_1) \\
 & + \frac{\lambda_1}{2} (\Phi_1^\dagger \Phi_1)^2 + \frac{\lambda_2}{2} (\Phi_2^\dagger \Phi_2)^2 + \lambda_3 \Phi_1^\dagger \Phi_1 \Phi_2^\dagger \Phi_2 \\
 & + \lambda_4 \Phi_1^\dagger \Phi_2 \Phi_2^\dagger \Phi_1 + \frac{\lambda_5}{2} [(\Phi_1^\dagger \Phi_2)^2 + (\Phi_2^\dagger \Phi_1)^2]. \quad (1)
 \end{aligned}$$

As free parameters, one can use the four scalar masses, along with  $\alpha$ ,  $\beta$ , and  $\mu^2$ . In terms of these parameters, one finds [39]

$$\lambda_1 = \frac{1}{v^2 \cos^2 \beta} (\cos^2 \alpha M_{H^0}^2 + \sin^2 \alpha M_{h^0}^2 - \mu^2 \tan \beta) \quad (2)$$

where  $v = 246 \text{ GeV}$ . If one considers the  $Z_2$  symmetric case, then  $\mu^2 = 0$ , and this leads, since  $M_{H^0}^2 > M_{h^0}^2$ , to a lower bound on

$$\lambda_1 > 0.25(1 + \tan^2 \beta). \quad (3)$$

Clearly, for large  $\tan\beta$ ,  $\lambda_1$  becomes nonperturbative. Requiring  $\frac{\lambda_1}{4\pi} < 1$  implies  $\tan\beta < 7$ . We therefore concentrate on this region of relatively small  $\tan\beta$ . However, if  $\mu^2 \neq 0$ , then parameters can be chosen to avoid this constraint, although some fine-tuning is then required.

### III. CONSTRAINTS FROM HEAVY HIGGS SEARCHES

ATLAS and CMS have obtained upper bounds on a Standard Model Higgs boson with a mass between 150 and 600 GeV and assuming a Standard Model width. We use the 95% confidence level band from recent CMS bounds (from Fig. 11 in Ref. [40]) and scale predictions as the inverse square root of the integrated luminosity.

For example, suppose  $M_{H^0}$  is 200 GeV. A Standard Model Higgs boson of 200 GeV will decay almost 100%

of the time into vector bosons. This is also true (except for extreme values of the parameters) in a 2HDM. The production rate through gluon fusion in the 2HDM will be different than the Standard Model rate because of the different  $t$  and  $b$  couplings. Thus, the upper bound from ATLAS and CMS on the cross section relative to the Standard Model rate will place a constraint on  $\alpha$  and  $\beta$ .

For  $M_{H^0} = 200$  GeV, we find the results in Fig. 2. We show results for the type-I and type-II models, with the current limits and projections for  $300 \text{ fb}^{-1}$  and  $3000 \text{ fb}^{-1}$ . The lepton-specific and flipped models give very similar results to the type-I and type-II models, respectively. An increase in luminosity will tightly constrain  $\cos(\beta - \alpha)$  for  $\tan \beta < 4$  in the type-I model and will give a significant constraint for  $\tan \beta < 4$  in the type-II model. In Fig. 3, we compare current limits from measurements of light Higgs decays with the limits obtained from the heavy Higgs search. We see that even with current bounds, a significant fraction of the previously allowed parameter space in the type-I model is excluded by the heavy Higgs search results, and this fraction grows with increasing integrated luminosity (unless, of course, the heavy Higgs is discovered). For the type-II model, some of the remaining parameter space is excluded, especially for small  $\tan \beta$ . This is a significant result, and shows that the allowed parameter space of a 2HDM can be substantially narrowed by considering bounds from heavy Higgs searches.

Once the mass of the heavy Higgs,  $H^0$ , exceeds 250 GeV, then the decay  $H^0 \rightarrow h^0 h^0$  is allowed, which will suppress the branching ratio of the  $H$  into vector bosons. The decay width for  $H^0 \rightarrow h^0 h^0$  depends on  $\mu^2$ . For the moment, we consider the  $\mu^2 = 0$  limit of unbroken  $Z_2$  symmetry. The width is

$$\Gamma(H^0 \rightarrow h^0 h^0) = \frac{\lambda_{Hhh}^2}{8\pi M_H} \left(1 - \frac{4m_h^2}{M_H^2}\right)^{1/2} \quad (4)$$

where [41]

$$\lambda_{Hhh} = -\cos(\beta - \alpha) \left( \frac{\sin 2\alpha}{\sin 2\beta} \right) \frac{M_{H^0}^2 + 2M_{h^0}^2}{2v}. \quad (5)$$

Since the decay width of  $H^0$  into vector bosons also depends on  $\cos(\beta - \alpha)$ , this factor cancels in the branching ratio. The results from the exclusion of  $M_{H^0} = 300$  GeV are shown in Figs. 3 and 4. We see that, as expected due to the opening up of the  $H^0 \rightarrow h^0 h^0$  channel, the exclusion region in the type-I model is smaller than from  $M_H = 200$  GeV, but is still not insubstantial, and becomes quite significant at high integrated luminosity. In the type-II model, the only additional exclusion regions are at relatively low  $\tan \beta$ . Note the dip at  $\cos(\beta - \alpha)$  near zero—this occurs because in that limit, both  $H^0 \rightarrow VV$  and  $H^0 \rightarrow h^0 h^0$  vanish, leaving  $H^0 \rightarrow b\bar{b}$  as the dominant decay. The results for  $M_{H^0} = 400$  GeV are not shown. The additional parameter space excluded is restricted to a small region for small  $\tan \beta$  in the type-I and lepton-specific models. Clearly, the bounds for higher masses will be weaker.

In the above, we assumed that the  $\mu^2$  term, which softly breaks the  $Z_2$  symmetry, is absent. This is technically natural, and in many models the term is naturally small. If it is not small, however, it will affect our results. Including the term causes the  $Hhh$  coupling to be multiplied [41] by a factor of

$$\lambda_{Hhh} \rightarrow \lambda_{Hhh} \left\{ 1 - x \left( \frac{3}{\sin 2\beta} - \frac{1}{\sin 2\alpha} \right) \right\}, \quad (6)$$

where  $x \equiv 2\mu^2 / (M_{H^0}^2 + 2M_{h^0}^2)$ . In Fig. 5, we have shown, for the type-I model, how our results are modified as  $x$  is varied.

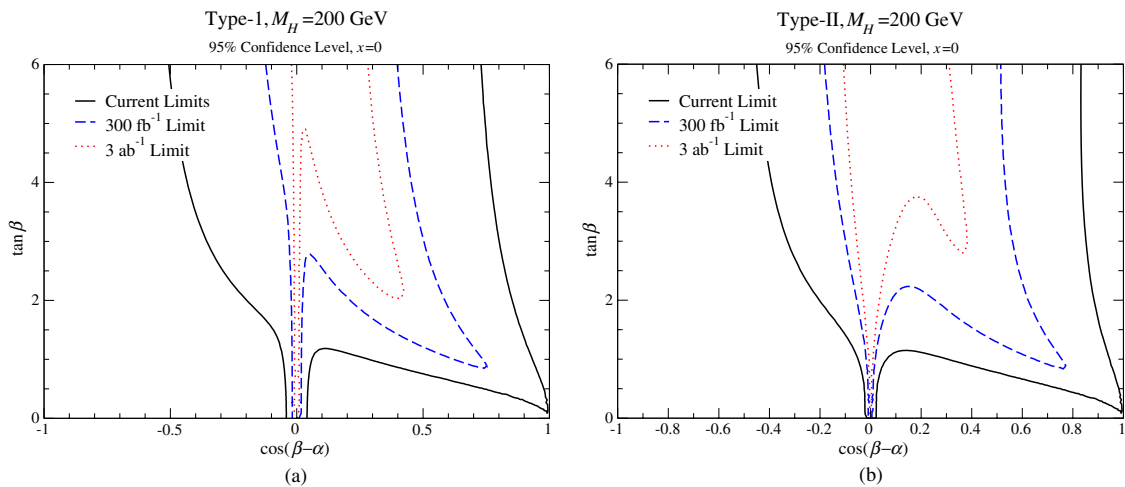


FIG. 2 (color online). Allowed regions in type-I (a) and type-II (b) 2HDMs from the LHC limit on a 200 GeV heavy Higgs boson. The region between the black (solid), blue (dashed), and red (dotted) curves is allowed at 95% confidence level corresponding to the current limits and the projected limits for integrated luminosities of  $300 \text{ fb}^{-1}$  and  $3000 \text{ fb}^{-1}$ , respectively.

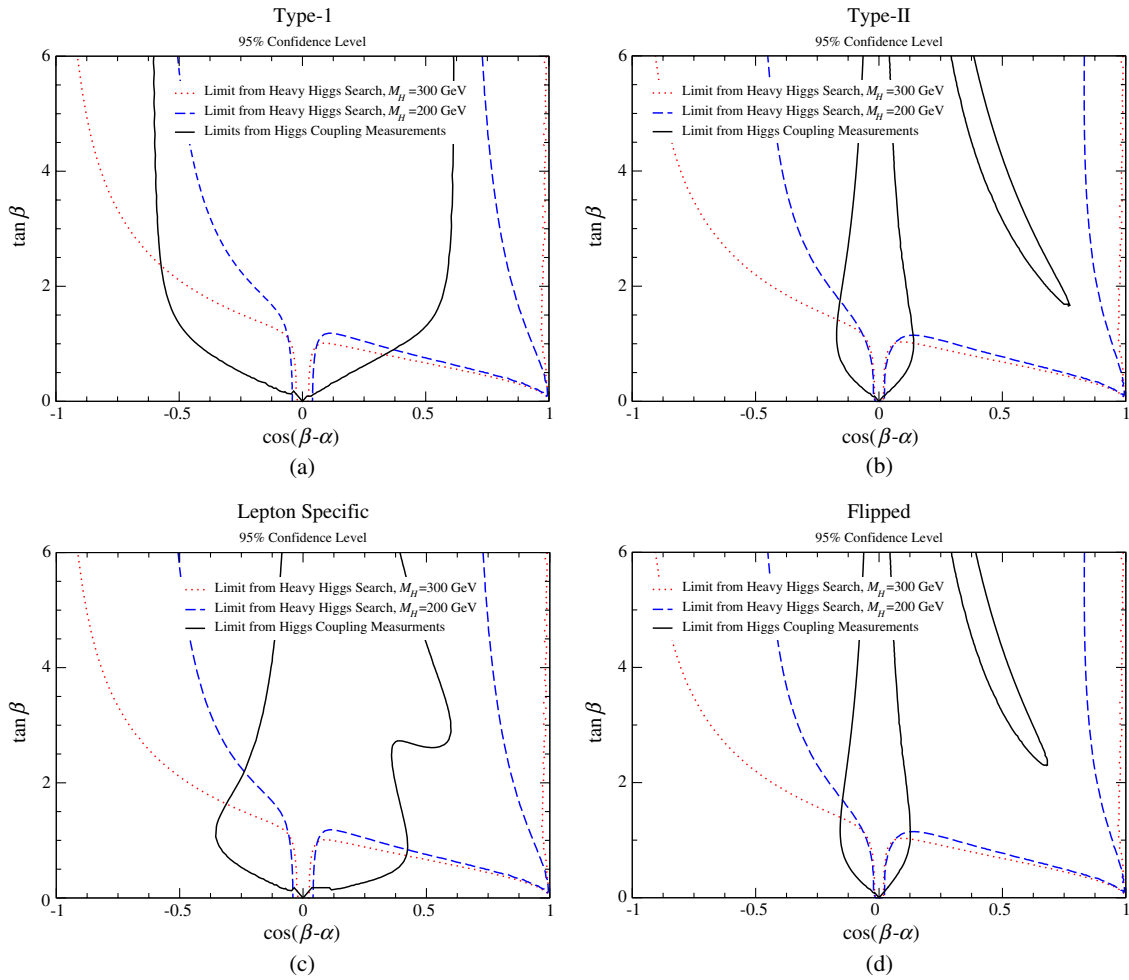


FIG. 3 (color online). Allowed regions in type-I (a), type-II (b), lepton-specific (c), and flipped (d) 2HDMs from the LHC limit on a 200 GeV and a 300 GeV heavy Higgs boson [blue (dashed line), red (dotted line)] and the current limits from light Higgs decays [black (solid line)].

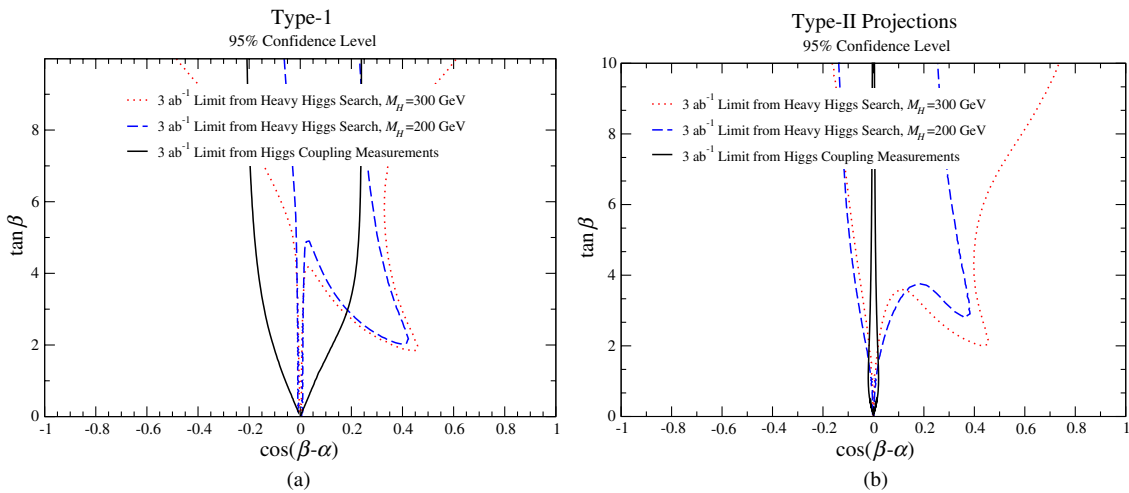


FIG. 4 (color online). Allowed regions in the  $(\cos(\beta-\alpha), \tan\beta)$  plane in type I (a) and type II (b) 2HDMs for a potential integrated luminosity of  $3 \text{ ab}^{-1}$ . The region between the black (solid), blue (dashed), and red (dotted) lines is allowed at 95% confidence level projected from the Higgs coupling measurements and the heavy Higgs search at  $M_{H^0} = 200$  and 300 GeV, respectively.

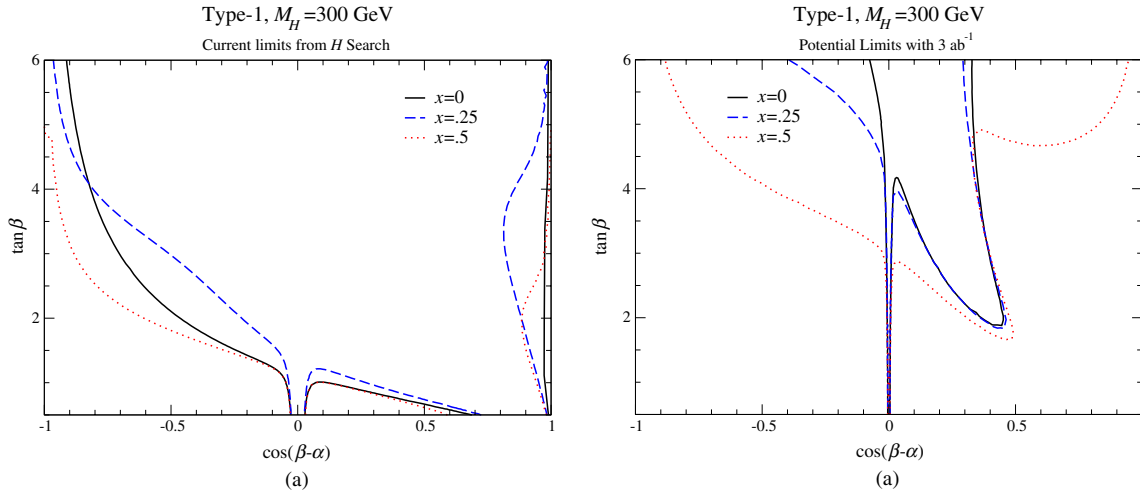


FIG. 5 (color online). Allowed regions in the  $(\cos(\beta - \alpha), \tan \beta)$  plane from the current limits found from the heavy Higgs search (a) and the projected limits for an integrated luminosity of  $3 \text{ ab}^{-1}$  (b) in the type-I 2HDM with  $M_{H^0} = 300$  GeV. In (a), the regions above the horizontal black (solid), blue (dashed), and red (dotted) lines and to the right of the vertical lines at small  $\cos(\alpha - \beta)$  are allowed at 95% confidence level corresponding to  $x = 0, 0.25,$  and  $0.5$ , respectively. In (b), the allowed regions are those above and enclosed by the curves.

#### IV. CONCLUSIONS

The discovery of the 125 GeV Higgs boson and the measurement of its branching ratios has initiated the exploration of the electroweak symmetry breaking sector. The implications of the discovery for the simplest extensions of the Standard Model, the two Higgs doublet models, have been extensively studied and the allowed regions of parameter space determined. In this paper, we examined the projected sensitivity of these analyses when the LHC acquired  $300 \text{ fb}^{-1}$  and  $3000 \text{ fb}^{-1}$  and demonstrated that LHC bounds on a heavy Standard Model Higgs (between 200 and 400 GeV) can further restrict the parameter space. In particular, for the type-I 2HDM with a heavy Higgs mass of 200 GeV,

the parameter space allowed from branching ratios of the 125 GeV Higgs can be shrunk by more than a factor of 2 by including bounds from the heavy Higgs searches. It is thus important, in the LHC upgrade, to continue these searches.

#### ACKNOWLEDGMENTS

We would like to thank Nathaniel Craig, Rui Santos, Scott Thomas and Gordon Watts for helpful discussions. The work of C.-Y.C. and S.D. is supported by the U.S. Department of Energy under Grant No. DE-AC02-98CH10886, and the work of M.S. is supported by the National Science Foundation under Grant No. NSF-PHY-1068008.

- 
- [1] G. C. Branco, P. M. Ferreira, L. Lavoura, M. N. Rebelo, M. Sher, and J. P. Silva, *Phys. Rep.* **516**, 1 (2012).
  - [2] P. M. Ferreira, R. Santos, M. Sher, and J. P. Silva, *Phys. Rev. D* **85**, 035020 (2012).
  - [3] A. Drozd, B. Grzadkowski, J. F. Gunion, and Y. Jiang, *J. High Energy Phys.* **05** (2013) 072.
  - [4] S. Chang, S. K. Kang, J.-P. Lee, K. Y. Lee, S. C. Park, and J. Song, *J. High Energy Phys.* **05** (2013) 075.
  - [5] P. M. Ferreira, R. Santos, M. Sher, and J. P. Silva, *Phys. Rev. D* **85**, 077703 (2012).
  - [6] C.-Y. Chen and S. Dawson, *Phys. Rev. D* **87**, 055016 (2013).
  - [7] D. S. M. Alves, P. J. Fox, and N. J. Weiner, [arXiv:1207.5499](https://arxiv.org/abs/1207.5499).
  - [8] N. Craig and S. Thomas, *J. High Energy Phys.* **11** (2012) 083.
  - [9] N. Craig, J. A. Evans, R. Gray, C. Kilic, M. Park, S. Somalwar, and S. Thomas, *J. High Energy Phys.* **02** (2013) 033.
  - [10] Y. Bai, V. Barger, L. L. Everett, and G. Shaughnessy, [arXiv:1210.4922](https://arxiv.org/abs/1210.4922).
  - [11] A. Azatov and J. Galloway, *Int. J. Mod. Phys. A* **28**, 1330004 (2013).
  - [12] B. A. Dobrescu and J. D. Lykken, *J. High Energy Phys.* **02** (2013) 073.
  - [13] P. M. Ferreira, H. E. Haber, R. Santos, and J. P. Silva, *Phys. Rev. D* **87**, 055009 (2013).
  - [14] A. Celis, V. Ilisie, and A. Pich, [arXiv:1302.4022](https://arxiv.org/abs/1302.4022).
  - [15] B. Grinstein and P. Uttayarat, [arXiv:1304.0028](https://arxiv.org/abs/1304.0028).
  - [16] M. Krawczyk, D. Sokolowska, and B. Swiezewska, [arXiv:1303.7102](https://arxiv.org/abs/1303.7102).
  - [17] B. Coleppa, F. Kling, and S. Su, [arXiv:1305.0002](https://arxiv.org/abs/1305.0002).

- [18] W. Altmannshofer, S. Gori, and G. D. Kribs, *Phys. Rev. D* **86**, 115009 (2012).
- [19] C.-W. Chiang and K. Yagyu, [arXiv:1303.0168](https://arxiv.org/abs/1303.0168).
- [20] L. Basso, A. Lipniacka, F. Mahmoudi, S. Moretti, P. Osland, G.M. Pruna, and M. Purmohammadi, *J. High Energy Phys.* **11** (2012) 011.
- [21] J. Chang, K. Cheung, P.-Y. Tseng, and T.-C. Yuan, *Phys. Rev. D* **87**, 035008 (2013).
- [22] N. Craig, J. Galloway, and S. Thomas, [arXiv:1305.2424](https://arxiv.org/abs/1305.2424).
- [23] A. Barroso, P.M. Ferreira, R. Santos, M. Sher, and J. Bo P. Silva, [arXiv:1304.5225](https://arxiv.org/abs/1304.5225).
- [24] CMS Collaboration, Report No. CMS Note 2012-006.
- [25] The assumption that the uncertainty scales as  $1/\sqrt{L}$  is true for the statistical error, and assumes that improvements are made in the systematic errors with increasing luminosity. This assumption is therefore optimistic, but is the one used by CMS for the European Strategy Report [24].
- [26] ATLAS Collaboration, Report No. ATLAS-CONF-2013-012.
- [27] CMS Collaboration, Report No. CMS PAS HIG-13-001.
- [28] See talk slides, “ $H \rightarrow b\bar{b}$  from Tevatron,” by Yuji Enari, at HCP2012.
- [29] ATLAS Collaboration, Report No. ATLAS-CONF-2013-030.
- [30] CMS Collaboration, Report No. CMS PAS HIG-13-003.
- [31] ATLAS Collaboration, Report No. ATLAS-CONF-2013-013.
- [32] CMS Collaboration, Report No. CMS PAS HIG-13-002.
- [33] ATLAS Collaboration, Report No. ATLAS-CONF-2012-170.
- [34] CMS Collaboration, Report No. CMS PAS HIG-12-044.
- [35] ATLAS Collaboration, Report No. ATLAS-CONF-2012-160.
- [36] CMS Collaboration, Report No. CMS PAS HIG-13-004.
- [37] F. Mahmoudi and O. Stal, *Phys. Rev. D* **81**, 035016 (2010).
- [38] N. Craig, J. Galloway, and S. Thomas, <https://indico.cern.ch/conferenceTimeTable.py?confId=248303#20130425>.
- [39] A. Barroso, P.M. Ferreira, I.P. Ivanov, and R. Santos, *J. High Energy Phys.* **06** (2013) 045.
- [40] CMS Collaboration, *Eur. Phys. J. C* **73**, 2469 (2013).
- [41] S. Kanemura, Y. Okada, E. Senaha, and C.-P. Yuan, *Phys. Rev. D* **70**, 115002 (2004).